Journal of Thermal Analysis and Calorimetry (2023) 148:1577–1580
https://doi.org/10.1007/s10973-022-11675-z

Temperature dependence of structural and magnetic transformations in Finemet-type amorphous alloys with Fe substituted for La

Marek Moneta[1] · Michał Wasiak[2] · Pavol Sovak[3]

Received: 1 November 2021 / Accepted: 27 September 2022 / Published online: 20 October 2022

Abstract
Structural and magnetic properties of amorphous and partly crystallized $Fe_{73.5-x}La_{x=0,1,3,5,7}Si_{13.5}B_9Nb_3Cu_1$ alloys were analysed in the temperature ranging from room temperature (RT) to 800 °C with differential scanning calorimetry (DSC) and thermomagnetic gravimetry (TMG). The Fe(Si) and Fe(B) structures were identified and characterized with set of crystallization temperatures and activation energies. Also, Curie temperatures for amorphous and for crystalline structures were determined and analysed as functions of La content.

Keywords Finemet alloys · La compounds · DSC · TMG

Introduction

Alloys, like $Fe_{73.5}Si_{13.5}B_9Nb_3Cu_1$ (at.%) classical Finemet, appear primarily in amorphous-magnetic phase, which after appropriate thermal or mechanical treatment, are transformed into the phase, when iron-silicides and iron-borides magnetic nano-crystals are embedded in an amorphous residual matrix [1–3]. For practical purpose, in order to obtain soft magnetic properties of the material, it is important to get size of nano-crystals, during primary crystallization, smaller than the exchange-correlation length.

So far, many different modifications of the basic FeSiB composition were analysed while searching for better technical properties [3, 4]. The analysis was focused rather on products of primary crystallization at lower annealing temperatures with less interest on the secondary crystallization.

In this work, mainly secondary crystallization at higher temperatures and its correlation to magnetization phenomena of $Fe_{73.5-x}La_{x=0,1,3,5,7}Si_{13.5}B_9Nb_3Cu_1$, (Finemet with Fe substituted for La) was analysed by means of differential scanning calorimetry (DSC) and performed at the same time, thermomagnetic gravimetry (TMG). Identification of structures and magnetic properties of the present alloys were based on our previous DSC, X-ray diffraction (XRD) and Mössbauer spectroscopy study [3, 4] of the alloys with dopants other than La.

Experimental

Samples were prepared by casting melt on a rapidly rotating copper wheel, thus cooling it at 10^7 K s^{-1} and solidifying in the form of 20-μm-thick and 1-mm-width bands of amorphous alloy. Composition of the samples was established through initial weighting and finally checked by analysing spectra presented in Fig. 1 measured and analysed with Amptek XRF spectrometer.

The DSC heat flow as scans functions of temperature was performed on Setaram DSC 111 at heating rates ranging from 1 to 20 K min^{-1} with samples of various (~ 20 mg) masses in the ambient N_2 environment.

The thermomagnetic (TM) measurement of material magnetization was simultaneously performed with Setaram-111 in TG-DSC mode. A small neodymium magnet was used to produce a magnetic field B≈ 0.75 mT around the sample and a magnetic field gradient $-\nabla B \approx 0.14$ mT cm^{-1} parallel to the sample surface. The temperature ranged from RT up to 1073 K (and backwards).

✉ Marek Moneta
marek.moneta@uni.lodz.pl

[1] Wydział Fizyki i Informatyki Stosowanej, Katedra Fizyki Ciała Sałego, Uniwersytet Łódzki, Pomorska 149, 90-236 Łódź, Poland

[2] Wydział Chemii, Katedra Chemii Fizycznej, Uniwersytet Łódzki, Pomorska 165, 90-236 Łódź, Poland

[3] Department Condensed Matter Physics, P.J.Śaf rik University Košice, Park Angelinum 9, 041-54 Košice, Slovakia

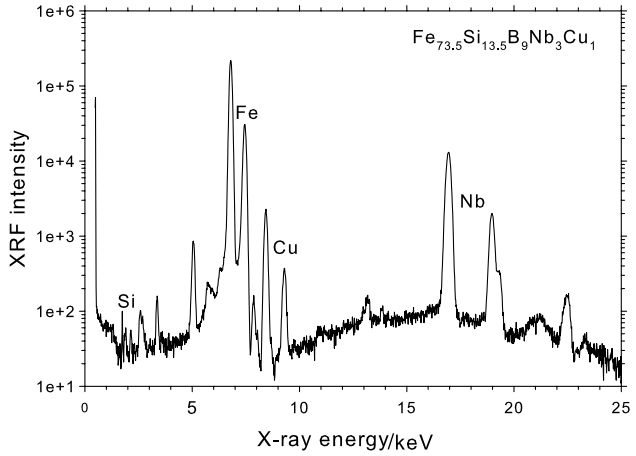

Fig. 1 XRF spectrum of pure Finemet measured in the air and analysed with Amptek spectrometer

Results and discussion

Calorimetry DSC

All DSC scans, which examples are shown in Figs. 2 and 3, display in fact two main structures, identified in the previous studies of the same basic alloy also with the use of XRD and Mössbauer spectroscopy [3, 4]. The first DSC peak corresponds to primary crystallization of silicides, mainly Fe_3Si with onset points at 450–480 °C in Finemet [1, 3]. The secondary structure is related to crystallization of borides, mainly Fe_3B and $Fe_{23}B_6$. In Finemet Fe_3B crystallizes at 540 − 600 °C [1, 3], whereas $Fe_{23}B_6$ precipitates at 400 °C and at 670–740 °C [5, 6]. Phase transfer parameters substantially depend on composition of the alloy and on details of thermal treatment.

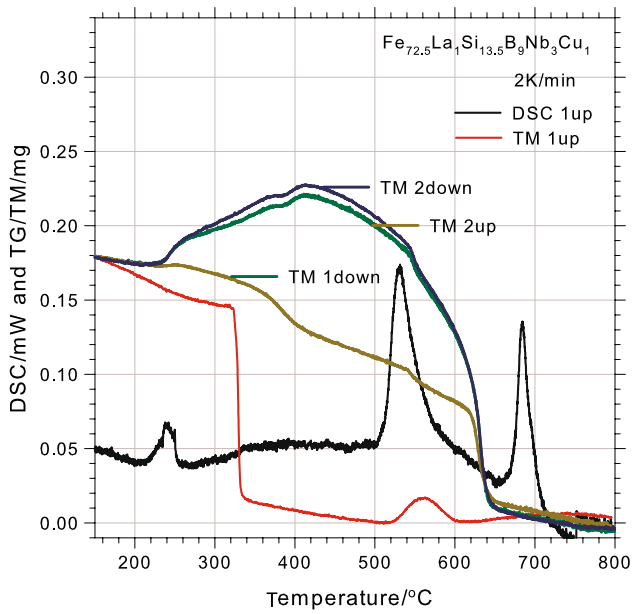

Fig. 2 (colour online) $Fe_{73.5-x}La_xSi_{13.5}B_9Nb_3Cu_1$ alloys. Examples of DSC and TM temperature scans at 2 K min^{-1} for $x = 1$ taken simultaneously. The scans during first heating of initial sample are shown with (1up). The next three curves represent subsequent TM scans for: first cooling (1down) second heating (2up) and second cooling (2down). The sample mass change $dm \sim 20$ μg corresponds to change of magnetization $dM \sim 1$ A m^{2}kg^{-1}

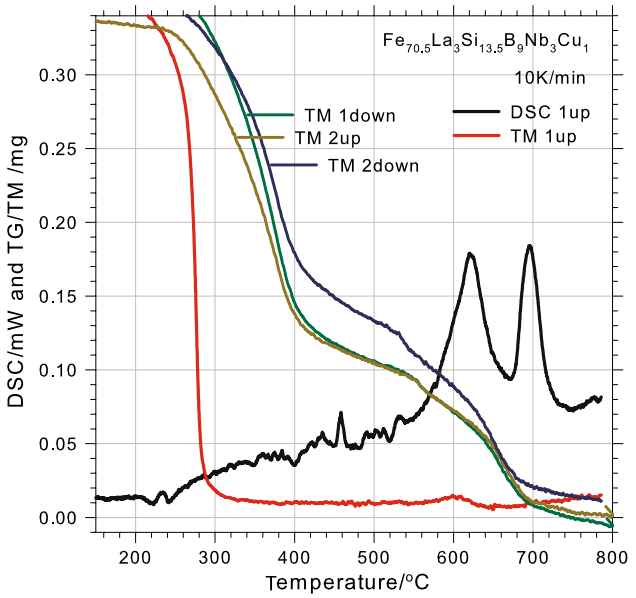

Fig. 3 As in Fig. 2, but at 10 K min^{-1} and for $x = 3$

For the present alloys, both primary and secondary crystallization onset points depend on the La content and generally addition of La shifts both peaks to higher temperatures. Increase in onset temperature for the peaks with the La content $x = 0 - 7$ and heating rate $v = 2$ and 10 K min^{-1} is presented in Fig. 4. The peaks are well resolved and allow us to calculate crystallization enthalpies and activation energies.

The effective activation energy for crystallization E_a can be determined from the Kissinger equation:

$$\frac{v}{T_p^2} = A \times \exp \frac{-E_a}{R \times T_p}, \tag{1}$$

where v is the temperature increase rate, $R = 8.31$ J mol^{-1} K^{-1} is the gas constant, T_p is the peak temperature and A is a constant. The activation energies E_a were calculated by fitting data points with Eq. (1). The calculated activation energy for primary crystallization of pure Finemet ($x = 0$) $E_a = 381$ kJ mol^{-1} corresponds to the value of 384 kJ mol^{-1} from Ref. [1]. The E_a values for $x = 0 - 7$ are presented in Fig. 5. As it is seen in the figure, E_a changes irregularly with La content x from 381 to 622 kJ mol^{-1} for primary

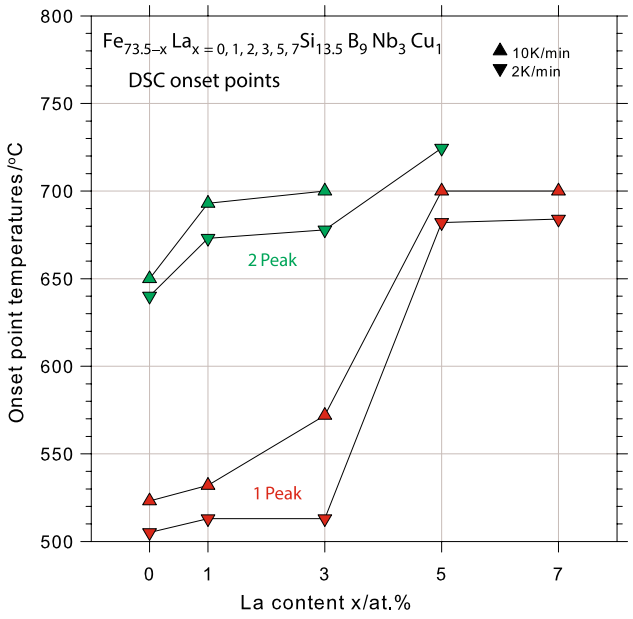

Fig. 4 (color online) Crystallization onset points for primary and secondary crystallization from DSC scans of $Fe_{73.5-x}La_{x=0,1,3,5,7}Si_{13.5}B_9Nb_3Cu_1$ alloys shown at heating rate of 2 K min^{-1} (∇) and 10 K min^{-1} (△)

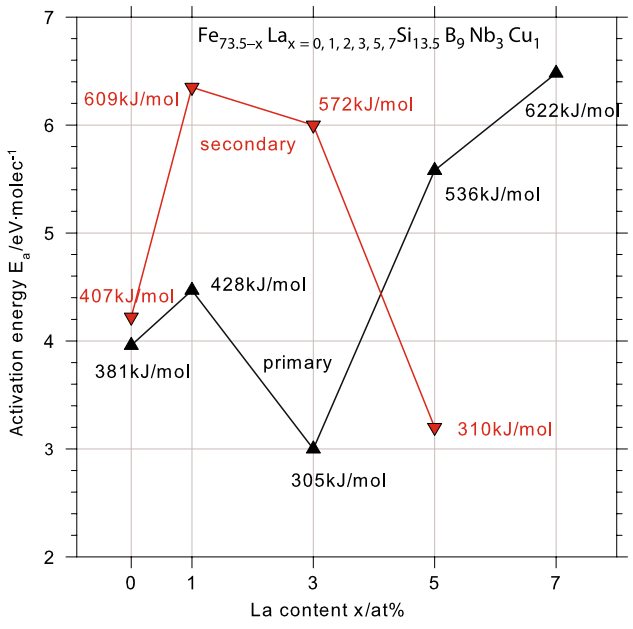

Fig. 5 (color online) $Fe_{73.5-x}La_{x=0,1,3,5,7}Si_{13.5}B_9Nb_3Cu_1$: activation energies E_a for primary (peak 1, △) and secondary (peaks 2, ∇) crystallization as shown in Figs. 2 and 3, in dependence on La content x, calculated from the Kissinger equation, Eq. (1)

crystallization and from 401 to 609 kJ mol^{-1} for secondary crystallization. This would suggest either more structures with empty nano-regions requiring energy-consuming rearrangement or an initial thermal treatment (or aging) of the amorphous alloy followed by precipitation of some Fe(Si) nanocrystals and enrichment of the residual amorphous phase with Nb and B, which makes further crystallization more difficult.

Magnetometry TM

Magnetization M was measured with TG via mass change dm, simultaneously with the corresponding DSC measurement. Scans of samples with La content $x = 1, 3$, heated at 2 and 10 K min^{-1}, are shown in Figs. 2 and 3 with thick black line. Initially, during the primary increase of temperature (TM 1up), M displays one abrupt fall to zero value. During the next three runs: when temperature decreases (TM 1down), then increases again (TM 2up) and finally decreases (TM 2down), the M scans run along similar curves, which reveal at least three characteristic regions. The scans were numerically deconvoluted with evolutionary algorithm [7], by fitting Brillouin functions in this regions to give the Curie temperatures in the range 350–380 °C, 500–550 °C and 630–750 °C, as it is shown in Fig. 6.

Physically, each alloy is initially amorphous and ferromagnetic and it remains amorphous up to the primary crystallization onset point reported in Fig. 4. The primarily amorphous phase losses ferromagnetic properties at the

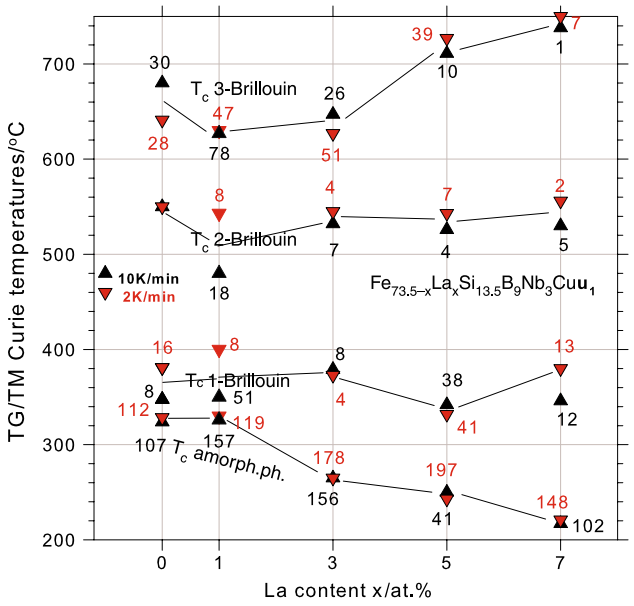

Fig. 6 (color online) $Fe_{73.5-x}La_{x=0,1,3,5,7}Si_{13.5}B_9Nb_3Cu_1$ alloys: Curie temperatures T_C for amorphous phase and for successive crystalline phases, in dependence on La content, as they appear in Figs. 2 and 3. T_C were obtained from fitting Brillouin functions to TG/TM scans measured at temperature increase rates 2 K min^{-1} (∇) and 10 K min^{-1} (△). Numbers next to the points refer to magnitude of magnetization change dM at the specified T_C via variation of the sample mass $-dm$ [μg]: $dm \sim 20$ µg corresponds to $dM \sim 1$ A m^2 kg^{-1}

Curie temperature of 300–200 °C, as is presented in Fig. 6. At this temperature, total magnetization of the sample drops by approximately $\delta M \approx$ 10–25 A m^2 kg^{-1}, as it is shown in Figs. 2 and 3 with thick red line (TM 1up). Pursuing further along TM curve, there is no magnetic response from the amorphous nonmagnetic matrix until crystalline structures are formed in correlation with exo-energetic peaks of crystallization on DSC scans in the figures. This means that some crystallization onset point temperature can be higher than the Curie temperature for the phase.

Magnetization of amorphous phase increases nearly linearly from approximately 5 to 10 A m^2 kg^{-1}, as the La content x changes from 0 to 7, as it is shown in Fig. 6 with the numbers at the experimental points given in μg mass units. Magnetization change of samples related next three crystalline structures and characterized by the Brillouin functions remain below 1 A m^2 kg^{-1} in dependence on La content x. The remaining magnetization of the sample at RT is up to 20% higher than the initial magnetization.

Since amorphous ferromagnets, similarly to crystalline ones, reveal spin wave excitations, the low-temperature magnetization $M(T)$ can be fitted with the Bloch equation:

$$\frac{\Delta M}{M(0)} = B \times T^{3/2} + C \times T^{5/2} \tag{2}$$

where $\Delta M = M(0) - M(T)$ and the B and C parameters of the order 10^{-5} K$^{-3/2}$ and 10^{-8} K$^{-5/2}$, respectively, were found by fitting the experimental data of magnetic scans with Eq. (2). Calculation of B and C allows us to determine the spin wave stiffness constants D$\approx 10^2$ meVÅ^2 and find the mean square ranges of exchange interaction $\langle r^2 \rangle \approx 10$ Å^2, considerably less than for crystalline ferromagnets. It implies a range of exchange interaction extending up to fourth or fifth nearest neighbours.

Also, it can be shown that close to the Curie temperature for amorphous phase the experimental data are better approximated by the Heisenberg model with the critical exponent $\alpha = 0.325$, than by the Weiss mean field model with $\alpha = 0.5$. This can be understood in terms of taking statistical average in the Heisenberg Hamiltonian H: in the Heisenberg model the spin correlations are taken into account and H contains terms $< s_i s_j >$, whereas in the mean field model the correlations are disregarded and H contains forms $< s_i >< s_j >$, where s_i,s_j are spins of the lattice sites i, j.

Conclusions

Properties of thin $Fe_{73.5-x}La_{x=0-7}Si_{13.5}B_9Nb_3Cu_1$ alloy foils were measured and analysed with complementary methods DSC and TM. Although the alloys crystallize in principle in two steps, the secondary crystallization reveals rather two tiny phases. The Curie temperature T_C for amorphous matrix reaches 320 °C for La-free alloy and drops to 220 °C for La-reach one, with $x = 7$. The Curie T_C for crystalline phases and also magnetization change at T_C do not substantially depend on La content.

Author Contributions Pavol Sovak prepared analysed materials. Michał Wasiak performed DSC and TM measurements. Marek Moneta performed TM measurements and prepared manuscript.

References

1. Chen WZ, Ryder PL. X-ray and differential scanning calorimetry study of the crystallization of amorphous $Fe_{73.5}Cu_1Si_{13.5}B_9Nb_3$ alloy. Mater Sci Eng. 1995;B34:204.
2. Antoszewska M, Wasiak M, Gwizdałła T, Sovak P, Moneta M. Thermal induced structural and magnetic transformations in $Fe_{73.5-x}Ce_{x=0,3,5,7}Si_{13.5}B_9Nb_3Cu_1$ amorphous alloy. J Therm Anal Calorim. 2014;115:1381–6.
3. Brzozowski R, Wasiak M, Piekarski H, Sovak P, Uznański P, Moneta M. Properties of Mn doped Finemet. J Alloys Compd. 2009;470:5.
4. Brzozowski R, Moneta M. Correlation between thermal induced structural and magnetic transformations in Si-rich $Fe_{73}Cu_1Si_{16}B_7Nb_3$ metal alloy Nucl. Instr Meth Phys Res. 2012;B279:208.
5. Long J, Ohodnicki PR, Laughlin DE, McHenry ME, Ohkubo T, Hono K. Structural Studies of Secondary Crystallization Products of the $Fe_{23}B_6$-type in a Nanocrystalline FeCoB-based Alloy. J Appl Phys. 2007;101:09N114.
6. Ponpandian N, Narayanasamy A, Chattopadhyay K, Manivel Raya M, Genesen K, Chinnasamay CN, Jeyadevan B. Low temperature magnetic properties and crystallisation behavior of finemet alloys. J Appl Phys. 2003;93:6182.
7. Gwizdałła TM, Moneta M. Mössbauer distribution fitting by using global optimization approach. Nucl Instrum Methods Phys Res. 2012;B279:205.